*16th World Conference on Earthquake Engineering, 16WCEE 2017*

*Santiago Chile, January 9th to 13th 2017*

*Paper N° 2579*

*Registration Code: S-P1461887441*

# LARGE-SCALE FSI EXPERIMENTS ON TSUNAMI-INDUCED FORCES IN BRIDGES

D. Istrati[(1)], I.G. Buckle[(2)], A. Itani[(3)], P. Lomonaco[(4)], S. Yim[(5)]

[(1)] *PhD Candidate, Department of Civil and Environmental Engineering, University of Nevada, Reno, distratii@unr.edu*
[(2)] *Foundation Professor, Department of Civil and Environmental Engineering, University of Nevada, Reno, igbuckle@unr.edu*
[(3)]*Professor, Department of Civil and Environmental Engineering, University of Nevada, Reno, itani@unr.edu*
[(4)] *Director, O.H. Hinsdale Wave Research Laboratory, Oregon State University, pedro.lomonaco@oregonstate.edu*
[(5)] *Professor, Department of Civil and Construction Engineering, Oregon State University, solomon.yim@oregonstate.edu*

## *Abstract*

Recent major earthquake events that occurred in the Indian Ocean (2004), Chile (2010) and Japan (2011) generated tsunami waves of significant heights, which inundated nearby coastal cities causing extreme destruction and loss of human lives. These waves inundated a large number of bridges, damaged the connections of the superstructure to the substructure in many cases and washed away the bridge decks. In the aftermath of these events the need to understand the tsunami effects and develop tsunami-resilient bridges in coastal communities became apparent.

In an attempt to cover the gap of knowledge, a series of large-scale experiments on tsunami waves impacting a bridge was recently conducted. This paper describes these experiments which were conducted in the Large Wave Flume at Oregon State University. The scale of the experiments were 1:5, which allowed for realistic modelling of an I-girder bridge with a concrete deck slab and four steel girders connected through shear studs to achieve composite behavior. The flexibility of the bridge connections and substructure was modeled explicitly using elastomeric bearings under each girder and springs at the level of the bent cap to represent the behavior of the substructure (columns). The same bridge model was tested under five different configurations of connections, switching from a flexible substructure to a rigid one and from elastomeric bearings to rigid ones, to gain insight into the physics of the dynamic fluid-structure-interaction. In this paper, results from the two first test cases are presented. In the experiments both solitary waves and bores of different heights and velocities were examined. Free-surface elevation, flow velocities and dynamic pressures were measured at certain locations along the flume as well as pressures on the bridge, connection forces, accelerations, strains and displacements.

It is shown that different phases exist in the vertical tsunami force histories, indicating (i) a large moment and a distinct rotational bridge mode at the time of the first impact of the tsunami wave on the bridge that induces the maximum tension in the offshore bearings, (ii) a pure uplift of the bridge during the passage of the wave through the bridge and (iii) a downward force at the end of the inundation. The maximum pressures on the offshore girder was seen to be up to 3.0 times larger than the pressures on the other girders. Furthermore, comparisons of the measured forces with integrated pressure measurements and inertial forces calculated from recorded accelerations, demonstrated the significance of the latter in satisfying the dynamic equilibrium of the bridge. Last, the ratio of maximum horizontal forces to maximum vertical forces was in the range of 0.54 to 2.2 and it was dependent on the wave type.

It is expected the data presented in this paper will be useful for evaluating the applicability and accuracy of proposed simplified equations for tsunami loads. It will also be valuable for hydrodynamic model calibration and validation and for determining the capability of existing numerical codes that simulate fluid-structure interaction effects in structures which have significant inertial effects and displacements.

*Keywords: tsunami; bridges; resilience, fluid-structure interaction; wave forces*

## 1. Introduction

In the last two decades humanity has witnessed large magnitude earthquakes with epicenters in the ocean, which generated tsunami waves of significant heights that caused unprecedented damage on coastal communities. Ports, buildings and infrastructure were severely damaged and bridges were washed away, cutting lifelines and hindering the efforts of rescue team to provide help to the people in need. In the 2011 Tohoku Mw 9.0 earthquake in Japan, many bridges were able to withstand the strong shaking, however approximately 100 of them failed due to the tsunami inundation [1]. The most severe and common type of failure in these bridges was the breaking of the connections between the superstructure and the substructure, which resulted in the unseating of the bridge deck by the tsunami waves (Fig. 1). These unforeseen events demonstrated the vulnerability of buildings and bridges to the tsunami waves and triggered the response of the society and research world in an attempt to improve the understanding of tsunami inundation and the effects on structures.

Fig. 1 – Damaged bridges after the 2011 tsunami in Japan: (a) Koizumi bridge on the left (from [1]) and (b) Tsuya railway bridge on the right (from [2])

Until recently, several interesting studies have been conducting including (i) on-site surveys and damage analysis [3, 4] (ii) small-scale experiments in wave flumes [5-11] and (iii) numerical model simulations [12-18]. On-site surveys analyzed the failed bridges and revealed that the possible failure mechanisms of bridges due to tsunami is scouring and overflow of bridge deck, where the latter can be either in the form of transverse drag due to large horizontal wave forces or in the form of overturning and uplift due to the combination of large vertical and horizontal tsunami forces [3].

Regarding the experimental studies, various researchers investigated the tsunami loads on flat slabs [5], box shaped bridge decks [6] and decks with girders [7-9] and in most cases both pressures and forces were measured. Most of these experiments were conducted at a small scale ranging from 1:100 to 1:35 and the bridge models consisted of acrylic or wood decks supported rigidly either from the top or the bottom of the deck. A larger scale (1:20) experiment was conducted in Japan [10] where several different cross-sections were examined, in an attempt to give insight into the forces that various types of bridges have to withstand and in this case the bridge model was rigidly supported on a pier. In general, two major issues with hydraulic experiments are (i) the inability to scale down the atmospheric pressure and (ii) the difficulty of scaling down properly the structural stiffness [18] indicating that scale effects can be significant in small-scale experiments. So far the largest scale experiment was conducted in [11] where they examined the performance of a 1.5 scaled pre-stressed bridge with rigid and flexible substructure, however the hydraulic tests were focused on hurricane waves and not tsunamis.

An alternative to the experimental studies, are the numerical simulations and several of them have been conducted to study tsunami force effects on bridges. These studies included mainly CFD analyses using various hydrodynamic codes such as FLOW3D [7], OpenFOAM [12-13] and CADMAS-SURF [14], where the bridge was modeled as a rigid boundary. The FEM-based multi-physics software LS-DYNA was also used in some studies [15-16] but the bridge material were still rigid. Most recently, advanced FSI analyses of an equivalent 2D bridge model with flexible deck and flexible connections was conducted in LS-DYNA [17] and the significance of the bridge dynamics and the dynamic FSI was shown. However, it was noted that due to the advanced nature of these multi-physics analyses the numerical results should be validated against experimental data.

## 2. Objective of this study

The fact that most of the experiments to date were conducted at a small scale using rigid models that could not account for the actual bridge dynamics and properties (material, flexibility, inertia) and the numerical simulations have limited validation or have been validated with small scale experiments where again the dynamic fluid-structure interaction was not considered, demonstrate the need for large scale hydraulic experiments of bridge models with realistic properties. Therefore, the main objective of this projects is to conduct at the largest possible scale hydraulic experiments of tsunami forces impacting a bridge with realistic behavior, where the flexibility of the superstructure, the substructure and the connections will be modeled, and obtain high quality data.

This data is expected to shed light on the physics of dynamic fluid-structure interaction and its effect on the tsunami forces that the bridge have to withstand, considering both the total forces and also the forces in each bearing. In addition, the experimental results can be used to examine the accuracy of empirical predictive equations for tsunami loads, calibration and validation of CFD models as well as validation of the FSI capabilities of numerical codes for structures with significant inertia effects and displacements. Furthermore, the data base can be the foundation for future development of recommendations and design codes for establishing tsunami-resilient bridges.

## 3. Experimental setup

### 3.1 Bridge description

Fig. 2 – Steel bridge after the assembly of steel components at Reno Iron works (left) and composite bridge sitting on the bent caps in the Large Scale Structures Lab at the University of Nevada, Reno (right)

For the hydraulic experiments conducted in this study a composite bridge model with four I-girders was designed and constructed at a 1:5 scale. The in-plane dimensions of the bridge deck are 3.45m length and 1.94m width. As shown in Fig.1 the steel girders are connected with cross-frames at the end supports and at third points. Two shear connectors of 0.95cm diameter have been welded on the flange of each girder every 5.1cm down the length of the girders in order to achieve the composite behavior with the deck which was constructed with concrete and is reinforced with a steel wire 4x4 - D5xD5. The thickness of the slab is 5.1 cm, the haunch is 1.0 cm and height of the steel girders is 21.3cm.

The bridge model was connected to the bent caps with two different type of connections, rigid spacers and plain elastomeric bearings to allow for thermal expansion. The bearing dimensions were 6.5 cm diameter and 1.27 cm height. Shear keys were also designed to take the lateral earthquake load and transfer it to the bent caps. The bearings and the shear keys correspond to realistic flexible connections which allow rotations and vertical displacements of the bridge but restrict the horizontal displacements. Rigid connections that restrained all the degrees of freedom were also designed and comparison with the previous case demonstrated the role of the flexibility of the connections. The bridge and the rest of the structural components were designed according to the AASHTO LRFD Bridge Design Specifications [19] assuming that the bridge was located in a Seismic Zone 3. The bridge and all the connecting elements were designed and constructed at the University of Nevada, Reno (Fig. 2) and then shipped to Oregon State University for testing in the Wave Flume.

## 3.2 Test facility, flume bathymetry and testing frame

The experiments were conducted in the Large Wave Flume (LWF) at the O.H. Hinsdale Wave Research Laboratory (HWRL) at Oregon State University. The flume is 104.24 m long, 3.66 m wide, and 4.57 m deep. The maximum depth for tsunami-type wave generation is 2 m, and the maximum wave height for this depth is 1.40m. The LWF is equipped with a piston-type dry-back wavemaker with a 4.2 m maximum stroke hydraulic actuator assembly and has a movable/adjustable bathymetry made of 20 square configurable concrete slabs. The flume includes a series of bolt-holes vertical patterns every 3.66m along the flume for supporting test specimens as well as the concrete bathymetry slabs.

For this project, parametric CFD analyses of the whole flume with the bridge were conducted in LS-DYNA [20] in order to identify the appropriate combination of slopes/bathymetry that will permit the testing of both unbroken and broken waves and determine the optimum location of the bridge in the flume. A slope of 1:12 at the beginning, followed by a horizontal bathymetry 40.2m long and another 1:12 slope at the end of the flume for dissipating waves was seen to be the most appropriate (Fig.3). The slope at the beginning will cause a decrease of the water depth which will influence the wave and as a result the wave height will increase during propagation due to shoaling and depending on the ratio of the wave height (H)/water depth (d) it can break and forms a bore. In addition, the optimum location for the bridge was between bays 14 and 15, in order to allow for the bore to form after the wave breaking and still inundate the bridge (Fig.3).

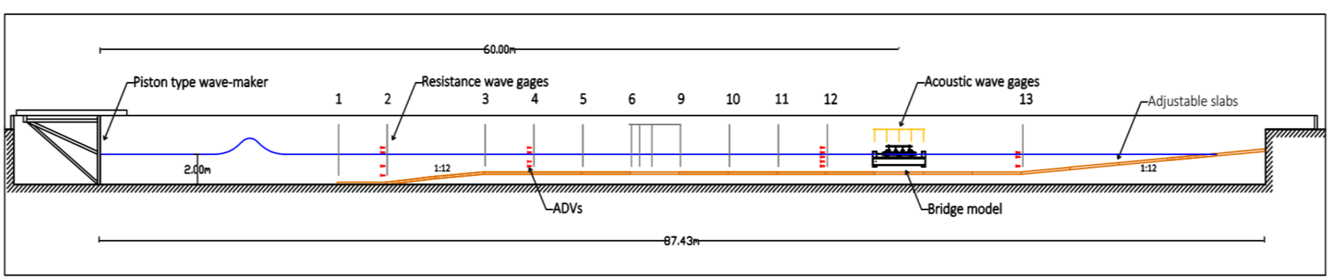


Fig. 3 – Cross-section of the flume depicting the bathymetry, bridge location and flume instrumentation

As can be seen in the Fig.4, the bridge was installed on the red bent caps which were supported by a testing frame consisting of two black beams and two brackets, which was bolted to the flume walls. The experimental setup also consisted of rails with small friction bolted on top of the black beams, carriages connected to the rails and the load cells below the red bent caps, load cells on top of the bent caps that were connected to the rigid spacers/bearings below the girders. The red bent caps and the testing frame was initially designed and used in [11] to study hurricane waves but had to be modified in order to be able to withstand the tsunami waves.

Fig. 4 – Installation of the bridge specimen on the bent caps (left) and bridge specimen connected to the red bent caps which were supported on the black test frame (right) in the Large Wave Flume at Oregon State University

### 3.3 Test cases – Wave Matrix

In the current experimental study, ten different configurations of a straight bridge and four configurations of a skew bridge, with a total of 280 tests were conducted. Five of these test cases were focusing on the effect of the dynamic fluid-structure interaction and these cases are shown in Table 1. Results from the first two cases are discussed in this paper. The differences between test cases ST1 and ST2 lies in the connection of the girder to the load cells on top of the bent caps, which in the former case is established with rigid spacers while in the latter this is done with elastomeric bearings (flexible). Test cases ST3 and ST4 are different than the two previous cases since the substructure flexibility is now modeled explicitly using a linear horizontal medium spring (flexible) and a soft spring (very flexible) respectively instead of a rigid rod, as a link between the bent cap and the grey bracket connected to the flume wall. These springs were first designed and used in [11], where the stiffness of the medium spring was selected to represent the scaled fundamental period of the prototype I-10 Bridge over Escambia Bay. The spring stiffness was 458 kN/m for the medium spring and 107kN/m for the soft spring. Last, test case ST11 was similar to case ST2 however the shear keys were removed and the bridge deck was allowed to move freely restricted only by the elastomeric bearings.

Table 1 – Test cases

| Case | Substructure | Girder Connections | Shear Keys |
|---|---|---|---|
| **ST1** | Rigid | Rigid | Yes |
| **ST2** | Rigid | Flexible | Yes |
| **ST3** | Flexible | Flexible | Yes |
| **ST4** | Very flexible | Flexible | Yes |
| **ST11** | Rigid | Flexible | No |

Several experimental studies that have been conducted so far to evaluate the tsunami forces on bridges, modeled the tsunami waves either as solitary waves or bores. The solitary waves are easier to study due to their closed-form mathematical description and steady wave-shape, however the broken waves/bores might be more representative of the reality. Therefore, in this study both types of waves were tested in order to examine the sensitivity of the bridge response to the different wave types. Therefore, based on the CFD analyses a wave matrix was carefully selected which included two different wave depths, 1.90m and 2.00m and a range of wave heights from 0.36m to 1.40m, shown in Table 1. Two snapshots of a bore impacting the bridge is shown in Fig. 5.

Table 2 – Wave Matrix

| **Water Depth (m)** | **Wave height (m)** | **Wave Type** |
|---|---|---|
| 1.90 | 0.46 – 0.65 | Unbroken |
| | 0.80 - 1.30 | Broken |
| 2.00 | 0.36 – 0.70 | Unbroken |
| | 0.90 – 1.40 | Broken |

Fig.5 – Bore slightly before (right) and slightly after (left) impacting the bridge specimen

## 3.4 Instrumentation

### 3.4.1 Flume Instrumentation

Wave hydrodynamics were measured in the experiments using resistive-type wave gages, acoustic probes, pressure gages and ADVs. In particular, 13 resistive-type wave gages were installed along the length of the flume (Fig.3) to measure the free-surface elevation and capture the propagation of the waves (shoaling, breaking). Moreover, 5 ultrasound gages were installed at the location of the bridge to track the overtopping process, and 16 Vectrino-II ADVs were installed at four different locations in order to measure the flow velocities and determine the velocity profile. In addition, two pressure gages were added at the same location with two velocity profiles.

### 3.4.2 Bridge Instrumentation

The bridge was extensively instrumented in order to measure the impact tsunami pressures and loads and record the bridge response. Therefore, 12 pressure gages were installed on the steel girders and also on the concrete deck to capture the impact pressures at certain locations as shown in Fig. 6. In addition, 3 biaxial accelerometers together with 2 vertical and 2 horizontal string pots were installed on top of the concrete deck, to capture the bridge response in the horizontal and vertical axis. The accelerometers were installed at three locations on the top surface of the bridge deck, two of which were next to the offshore and onshore lifting lugs and the vertical string pots were installed at similar locations so that both type of instruments can capture the rotation of the bridge. The horizontal string pots were attached to stiff tubes that were bolted to the two bent caps to measure their displacements (Fig.6).

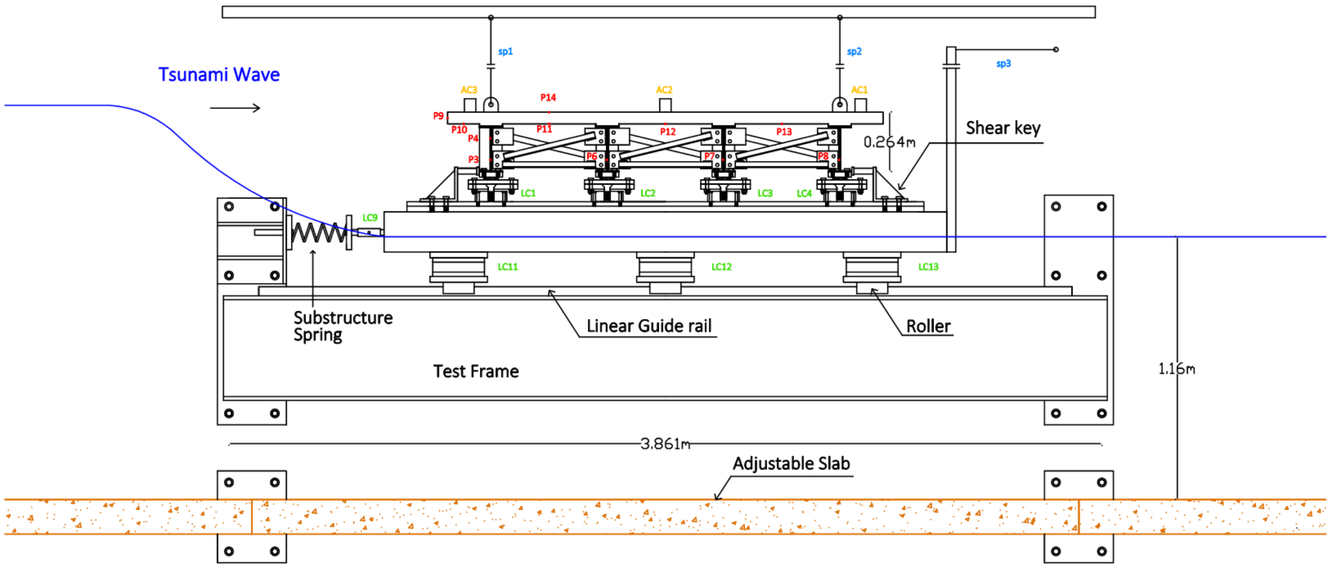


Fig. 6 – Cross-section of the experimental setup at the bridge location depicting the major components (test frame, bridge specimen, bent caps, connecting elements) and bridge instrumentation

Furthermore, eight submersible load cells were installed below the girders and six submersible load cells were installed below the bent cap in order to measure the vertical forces in the girder and bent cap connections respectively. These six submersible load cells were also used as a mean for examining the accuracy of the recorded total vertical tsunami forces applied to the bridge. Furthermore, two submersible load cells were installed horizontally at the level of the bent caps, to measure the total horizontal force transferred from the shear key to the bent caps and the supports. Apart from the above instruments, 24 strain gages were installed on the steel cross-frames in order to get an estimation of the forces carried by each member. The bridge instrumentation is shown in Fig.6.

## 4. Results

### 4.1 Test case ST1

This section will be focusing on representative experimental results for the first test case ST1. For validation purposes of the generated solitary waves in the LWF, the recorded free-surface elevation at the first wave gage is compared against the theoretical values predicted by the equation 7.155 shown in [21]. As it can be seen in Fig.7 the recorded free-surface elevation for the two different wave heights agree well with the theory. Fig. 8 is showing the wave propagation along the flume starting from wg2, which is located at the beginning of the flume and ending with wg13 which is located after the bridge. It can be interestingly noticed that the specific wave undergoes significant shoaling and the wave height increase by approximately 30% from wg2 to usg1which is located exactly before the bridge. In addition, the wg13 is showing significant decrease in the wave height after the impact on the bridge, indicating the loss of energy.

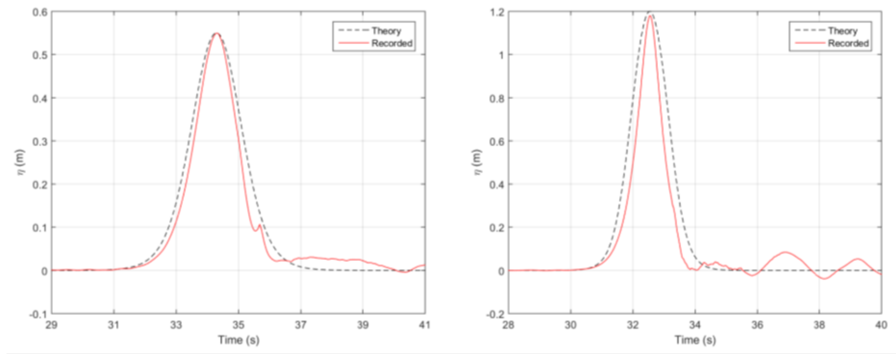


Fig.7 – Theoretical and recorded free-surface elevation at WG1 for H=0.55m (left) and H=1.20m (right)

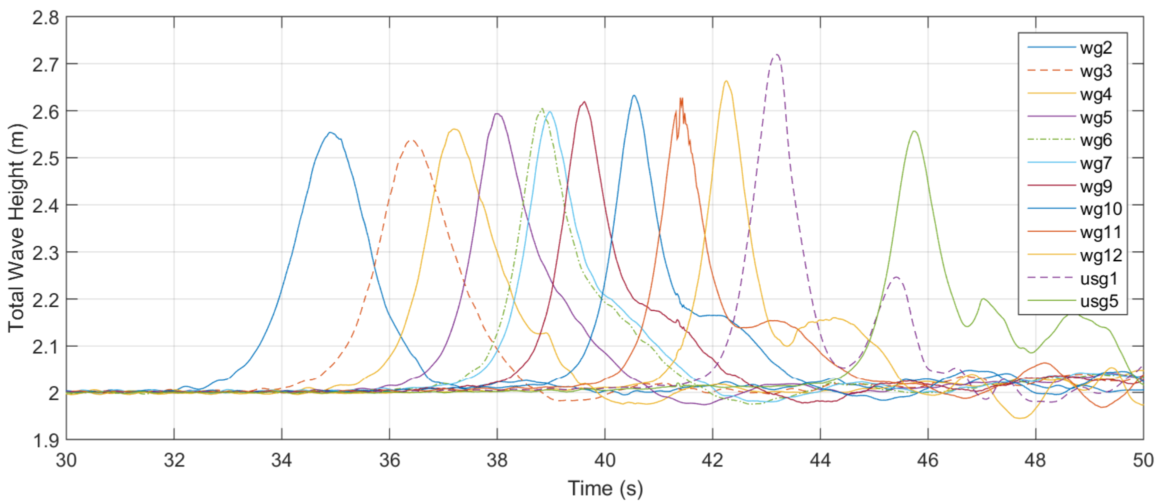


Fig.8 – Total wave heights at different locations along the flume for H=0.55m

In Fig. 9 (left) the vertical forces in the connections (rigid bearings) below each girder, as well as their summation, are plotted as a function of time. LC1+LC8 and LC4+LC5 are corresponding to bearings of the offshore and onshore girder respectively. Interestingly, in the force history, four different phases can be distinguished. Phase 1 is at the time of the first wave impact, where the offshore bearings are in tension (positive) and the onshore ones are in compression while the total vertical force is upwards (positive), indicating a large applied moment due to the applied horizontal and vertical tsunami load. Phase 2 is when the total vertical force becomes negative after the initial impact and then it fluctuates from negative to positive while the forces in some bearings have opposite signs than the others. Phase 3 has a longer duration that the first two phases and occurs when all bearings are going in tension indicating a governing vertical mode due to uplift. Phase 4 occurs towards the end of inundation when all bearings are in compression and the total vertical force is downward. This indicates that during the passage of the wave though the bridge, different structural modes are being excited, starting with a rotational mode along the longitudinal axis of the bridge at the time of the initial impact. This is due to the fact that the wave is a dynamic load that changes both magnitude and location in time. Until now, most of the researchers have been interested in the maximum total vertical load, however the experimental data in this study is indicating that attention should be given to the forces in the offshore bearings which are maximized during Phase 1. If the offshore bearings fail during Phase 1, then other bearings might follow, leading to a progressive collapse. The right side of Fig. 9 is showing the total vertical forces recorded in the girder and bent cap connections and the horizontal force recorded in the link. For this particular wave and test case the maximum horizontal force occurs at the time of the initial impact and its value is significantly smaller than the max vertical force. As expected, the total vertical forces recorded in the girder and bent cap connections have a good agreement, increasing therefore the confidence in the experimental data.

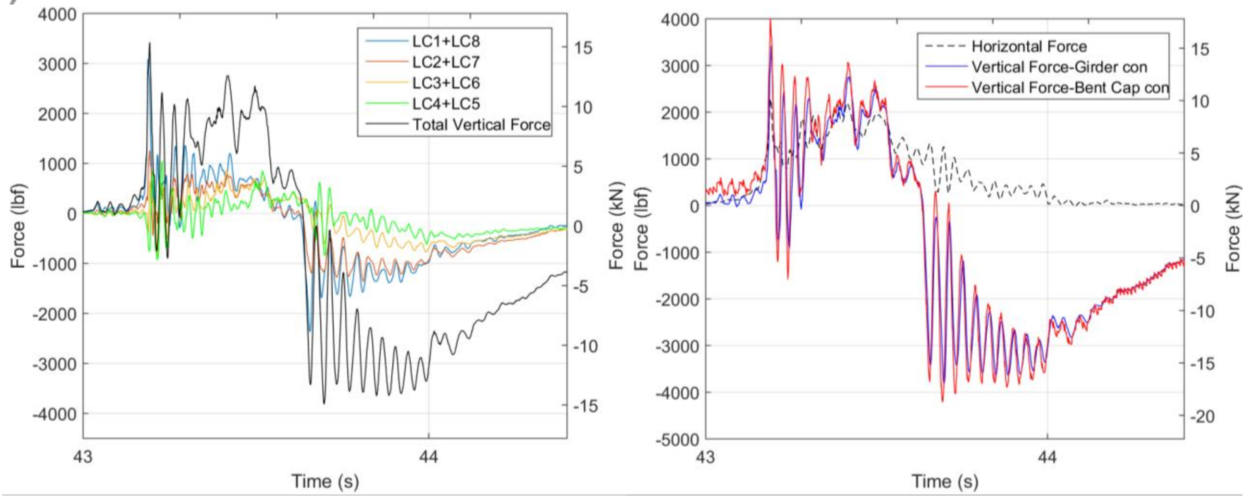


Fig. 9 –Vertical forces in the girder connections (left) and total horizontal & vertical forces (right) for H=0.55m

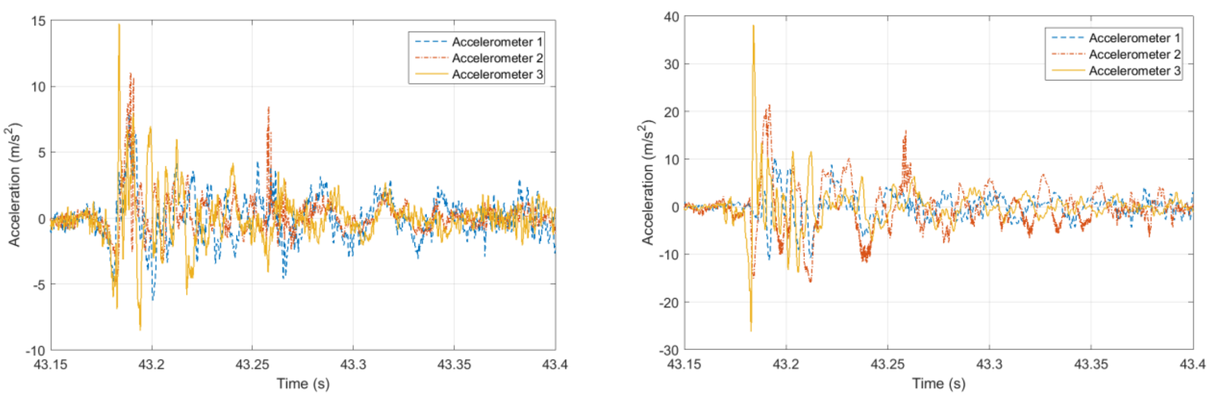


Fig.10 –Bridge accelerations in x direction (left) and z direction (right) for ST1 and H=0.55m

To better understand the dynamic fluid-structure interaction of the bridge with the tsunami wave, the horizontal (x-direction) and vertical accelerations (z-direction) of the bridge were plotted in Fig. 10. The vertical accelerations reached a maximum value of approximately 38 m/s$^2$, while the horizontal accelerations were significantly smaller that the vertical ones and reached a max value of 15 m/s$^2$. It is worth noting that the rotational vibration bridge mode noticed in the recorded force histories can also be observed in the vertical accelerations, since slightly after the initial impact the offshore accelerometer (accel. 3) is out of phase with the other accelerometers installed at the middle of the deck and the onshore side.

Fig. 11 (left) shows the horizontal pressure measured in the four girders for a sample of unbroken and broken waves. Girder1 corresponds to the offshore girder and girder 4 to the onshore. This graph clearly shows that the pressure on the offshore girder is significantly larger than the pressures of the other girders and it can actually be up to 3 times larger. Same figure on the right, shows the maximum recorded horizontal and vertical forces for all the unbroken and broken waves tested for case ST1. It can be clearly seen that the unbroken and broken waves introduce a different pattern of forces in the bridge connections. For the broken the horizontal forces tend to be larger than the vertical ones up to a factor of 2.2, while for the unbroken waves the opposite happens and the same factor can get down to 0.54. Therefore, it’s highly important to be able to identify the wave type to which the bridge will be subjected in order to be able to design the connections of a new bridge or strengthen the connections of an existing bridge appropriately.

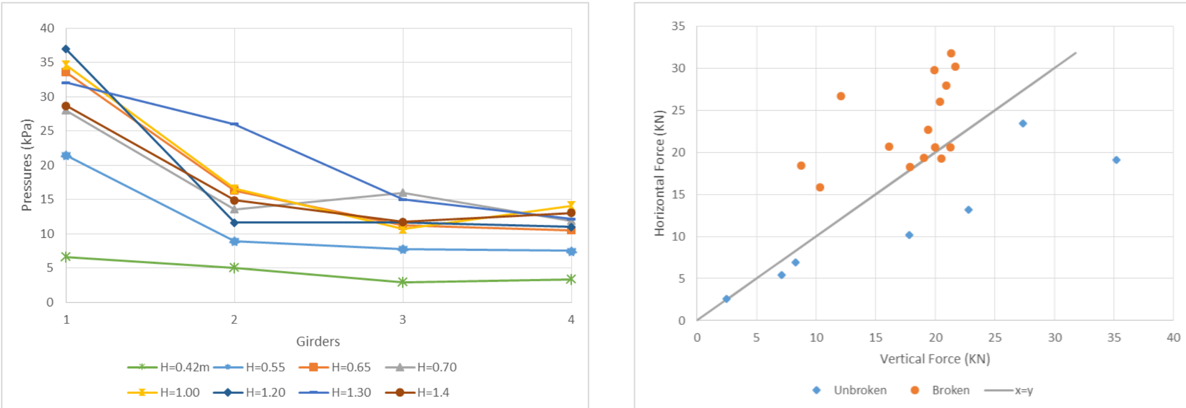


Fig.11 – Maximum recorded pressures on the girders (left) and maximum horizontal vs maximum vertical tsunami forces for test case ST1

## 4.2 Test Case ST2 - Effect of Inertia

The recorded accelerations of the bridge deck were used for calculating the inertia forces (effective mass times the recorded acceleration) and the pressure gages were integrated over the bridge to calculate the external tsunami load. The results for ST2 are plotted in Fig. 12 and very interesting conclusions can be drawn. On the left graph the horizontal external load and the recorded link forces are plotted as a function of time and significant differences can be observed between the two curves. The link does not have a peak force at the initial impact and is shows more fluctuations than the external load. One main reason for the observed difference might be the small number of pressure gages that were used for the calculation of the external load and the fact that they were installed only on the offshore face of each girder. The other reason is the fact that these two forces should be equal only in a static equilibrium (Fx, external = Fx, link) or a dynamic equilibrium (Fx, external = Fx, link + Fx, inertia) with negligible inertia forces. Therefore, on the right graph the inertia forces were added to the recorded link forces and a good agreement with the external load occurred at the beginning of the inundation. This is an extremely important new finding because it shows that the inertia forces cannot be neglected because they are large at the initial impact and play a significant role in satisfying the dynamic equilibrium of the bridge. Additional information about the role of inertia and the dynamic fluid-structure interaction can be found in [22].

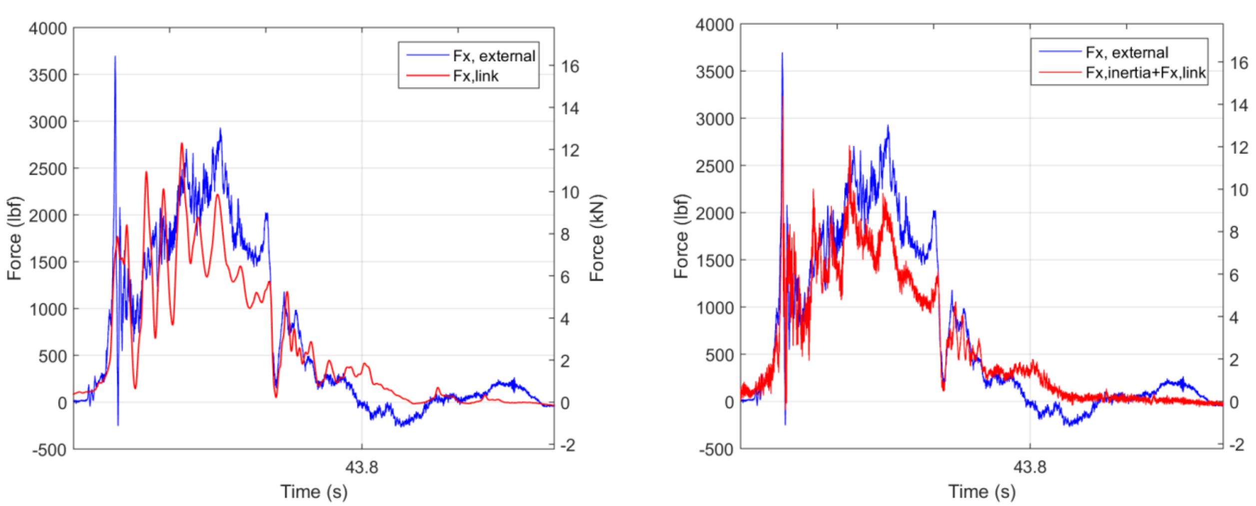


Fig.12 – Horizontal tsunami forces for test case ST2 and H=0.55m

## 5. Conclusions

The large scale hydraulic experiments described in this paper with the detailed measurements of the wave propagation and profile and the extensive instrumentation of the bridge with different type of instruments, provided high quality data that can prove useful for understanding the tsunami effects on bridges. Preliminary examination of the data has shown that:

Four different phases seem to exist in the vertical force histories, among which (i) a phase with a large moment and a distinct rotational bridge mode at the time of the first impact of the tsunami wave on the bridge, (ii) a phase with a pure uplift of the bridge during the passage of the wave through the bridge and (iii) a phase with a downward force towards the end of the inundation. Special attention should be given to phase 1 because it introduced the largest tension in the offshore bearings.

The recorded accelerations on the bridge deck showed peak values at the beginning of the inundation. The peak vertical acceleration was approximately 38 $m/s^2$ which was significantly larger than the peak horizontal acceleration of $15 m/s^2$ for a wave height of 0.55m.

The pressures on the offshore girder reached a maximum value of 37kPa. The maximum pressure on each girder was seen to depend on the wave height, however for all the waves the pressure on the offshore girder was consistently higher than the pressures on the other girders, up to a factor of 3.

The unbroken and broken waves introduced a different pattern of forces in the bridge connections. For the broken waves the ratio of maximum horizontal to maximum vertical force was larger than 1.0 for most waves and reached a maximum value of 2.2, while for the unbroken waves this ratio was smaller than 1.0 with a minimum value of 0.54. Therefore, it is important to be able to identify the wave type to which the bridge will be subjected.

The summation of horizontal inertia forces calculated from the measured accelerations and the measured link forces matched well the histories of the external tsunami load from integrated pressures, especially at the beginning of the inundation showing that the dynamic equilibrium was satisfied. This comparison revealed that at the time of the initial impact a large percentage of the short duration horizontal tsunami load is taken by the inertia forces, however later on the loads are mainly taken by the link.

The agreement of the horizontal inertia forces plus the link forces with the external tsunami load, as well as the agreement of the total vertical force recorded in the bearings with the total vertical force recorded in the bent cap connections increases the confidence in the validity of the recorded data.

## 6. Acknowledgements

This research project was funded by Federal Highway Administration under Contract No. DTFH61-07-C-0031. Authors wish to thank Tao Xiang, Tim Maddux and the staff of Hinsdale Wave Research Laboratory at Oregon State University for their assistance during the experiments.

## 7. Copyrights



## 8. References

[1] EERI Special Earthquake Report-October 2011. Learning from Earthquakes: Bridge Performance in the Mw 9.0 Tohoku, Japan, Earthquake of March 11, 2011.

[2] Yashinski M. http://www.bridgeofweek.com/ website.

[3] Kawashima K (2012): Damage of bridges due to the 2011 Great East Japan Earthquake. *Proc Int Symp on Engineering Lessons Learned from the 2011 Great East Japan Earthquake, March 1-4, 2012*, Tokyo, Japan.

[4] Kosa K (2012): Damage analysis of bridges affected by tsunami due to Great East Japan Earthquake. *Proc Int Symp on Engineering Lessons Learned from the 2011 Great East Japan Earthquake, March 1-4, 2012*, Tokyo, Japan.

[5] Seiffert B, Hayatdavoodi M, Ertekin, RC (2014): Experiments and computations of solitary-wave forces on a coastal-bridge deck. Part I: flat plate. *Coastal Engineering, 88, 194-209.*

[6] Hayashi H (2013): Study on tsunami wave force acting on a bridge superstructure. *Proc 29th US-Japan Bridge Engineering Workshop*, Tsukuba, Japan.

[7] Lau TL, Ohmachi T, Inoue S, Lukkunaprasit P (2011): Experimental and Numerical Modeling of Tsunami Force on Bridge Decks*. DOI: 10.5772/23622.*

[8] Maruyama K, Tanaka Y, Kosa K, Hosoda A, Mizutani N, Nakamura T (2013): Evaluation of tsunami force acted on bridges by Great East Japan Earthquake. *10 CUEE Conference Proceedings,* Tokyo, Japan.

[9] Hayatdavoodi M, Ertekin RC (2015b): Wave forces on a submerged horizontal plate. Part II: Solitary and cnoidal waves. *J.Fluids and Structures, 54(April), pp. 580–596.*

[10] Hoshikuma J, Zhang G, Nakao H, Sumimura T (2013): Tsunami-induced effects on girder bridges. *Proceedings of the International Symposium for Bridge Earthquake Engineering in Honor of Retirement of Professor Kazuhiko Kawashima,* Tokyo, Japan.

[11] Bradner C, Schumacher T, Cox D, Higgins C (2010): Experimental setup for a large-scale bridge superstructure model subjected to waves. *Journal of waterway, port, coastal, and ocean engineering, 137(1), pp. 3–11.*

[12] Hayatdavoodi M, Ertekin RC (2015a): Wave forces on a submerged horizontal plate. Part I: Theory and modelling. *J. Fluids and Structures, 54(April), pp. 566–579.*

[13] Bricker JD, Nakayama A (2014): Contribution of trapped air, deck superelevation, and nearby structures to bridge deck failure during a tsunami. *Journal of Hydraulic Engineering, 140(5), 05014002.*

[14] Kataoka S, Kaneko M (2013): Estimation of Wave Force Acting on Bridge Superstructures due to the 2011 Tohoku Tsunami. *Journal of Disaster Research Vol. 8.*

[15] Yim SC, Boon-intra S, Nimmala SB, Winston HM, Azadbakht M, Cheung, KF (2011): Development of a Guideline for Estimating Tsunami Forces on Bridge Superstructures. *Oregon Dept of Transportation Report No. OR-RD-12-03.*

[16] Azadbakht, Mohsen (2013): Tsunami and hurricane wave loads on bridge superstructures. *PhD dissertation,* Oregon State University.

[17] Istrati D, Buckle IG (2014): Effect of fluid-structure interaction on connection forces in bridges due to tsunami loads. *Proceedings of the 30th US-Japan Bridge Engineering Workshop,* Washington DC, United States.

[18] Martinelli L, Lamberti A, Gaeta MG, Tirindelli M, Alderson J, Schimmels S (2010): Wave Loads on Exposed Jetties: Description of Large-Scale Experiments and Preliminary Results. *Proc of the Int Conference on Coastal Eng; No 32.*

[19] AASHTO LRFD Bridge Design Specifications (2012). ISBN: 978-1-56051-523-4, Publication Code: LRFDUS-6.

[20] Hallquist JO (2014): LS-DYNA Theoretical Manual. Livermore Software Technology Corporation, Livermore, CA

[21] Hughes SA (1993): Physical models and laboratory techniques in coastal engineering. *Advanced Series on Ocean Engineering, Vol. 7, World Scientific Publishing,* Singapore.

[22] Istrati D, Buckle IG, Lomonaco P, Yim S, Itani A (2016): Large-scale Experiments of Tsunami Impact Forces on Bridges: The Role of Fluid-Structure Interaction and Air-venting. *Proceedings of the 26th (2016) International Ocean and Polar Engineering Conference, June 26-July 2, 2016,* Rhodes, Greece.